Robust Moving Path Following Control for Robotic Vehicles: Theory and Experiments

Matheus F. Reis, R. Praveen Jain, A. Pedro Aguiar and João Borges de Sousa

***Abstract*— This paper addresses the Moving Path Following (MPF) motion control problem that consists of steering a robotic vehicle along a specified geometric path expressed with respect to a *moving* target frame. External disturbances that depend on the operational environment such as maritime currents, wind or rough terrain can affect the vehicle motion in a variety of ways. Further, imperfections and simplifications of the vehicle model can also lead to unknown disturbances. One way to overcome this problem is by designing robust controllers to perform the task. Existing literature on MPF control does not consider these disturbances and further assume that the linear and angular velocity of the target frame is known. In this paper, these assumptions are relaxed through the design of robust MPF control schemes. To this end, two robust control strategies are proposed to solve the MPF control problem for a robotic vehicle with actuation constraints and bounded disturbances. Using Lyapunov-based arguments, both controllers are proven to be Globally Asymptotically Stable with respect to the origin of the MPF error. Experimental results using Autonomous Underwater Vehicles demonstrate the viability of the proposed control schemes for applications in a real world environment.**

I. INTRODUCTION

Two main approaches concerning the motion control for robotic vehicles are Trajectory Tracking and Path Following schemes [1], [2], [3], [4]. In trajectory tracking control, temporal constraints are explicitly defined for the vehicle motion, while the path following schemes require the vehicle to follow a geometric path without the need of satisfying explicit time constraints. This paper considers a generalization of the path following problem, termed the Moving Path Following (MPF) motion control problem. The MPF motion control problem consists of steering the robotic vehicle along a priori specified geometric path expressed with respect to a moving target frame. Such a problem finds applications in scenarios such as convoy protection, marine life tracking, etc. Further, the MPF problem retains all the characteristics of the classical path following schemes [5] such as faster convergence of the robot to the moving path.

This work was supported in part by the European Unions Horizon 2020 research and innovation programme MarineUAS under the Marie Sklodowska-Curie grant agreement No 642153, and projects IMPROVE - POCI- 01-0145- FEDER-031823, HARMONY, POCI-01-0145-FEDER-031411 - both funded by FEDER funds through COMPETE2020 - POCI and by national funds (PIDDAC), STRIDE - NORTE-01-0145-FEDER-000033, supported by NORTE2020, under the Portugal2020, through the European Regional Development Fund (ERDF), and SYSTEC - UID/EEA/00147/2019 - funded by national funds through FCT/MCTES (PIDDAC). A. Pedro Aguiar received a Sabbatical grant from FCT.

Matheus F. Reis, R. Praveen Jain, A. Pedro Aguiar and João Borges de Sousa are with the Department of Electrical and Computer Engineering, Faculty of Engineering, University of Porto, 4200-465 Porto, Portugal {matheusreis, praveenjain, pedro.aguiar, jtasso}@fe.up.pt

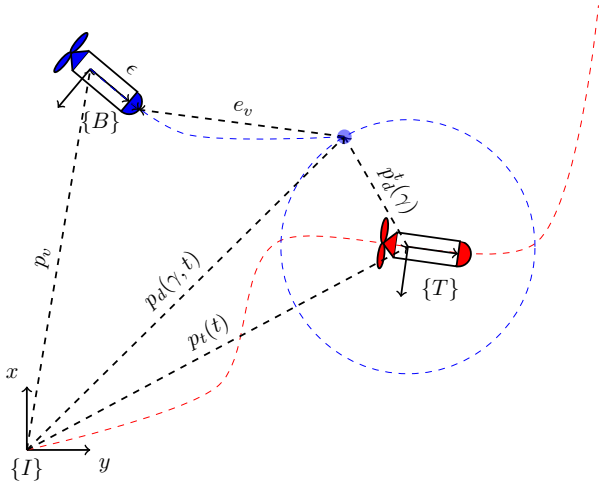

Fig. 1. Illustration of the MPF scenario and coordinate frames.

The MPF control problem was first introduced in [6], [7] for tracking of ground targets using Unmanned Aerial Vehicles (UAVs) in 2D case. An extension to the 3D case was presented in [8]. The proposed MPF approach was suitable for robotic vehicles such as UAVs that require a minimum positive forward speed for its operation. For robotic vehicles without such a restriction, a Lyapunov-based MPF control approach was presented in [9] for a translating target frame. Other control methods such as the vector field method [10] and nonlinear model predictive control [11] have been proposed to solve the MPF problem for unicycle type robots. The limitations of the existing literature in MPF control include: (i) the assumption that the pose and velocities of the target frame are known accurately and (ii) not explicitly considering the influence of external disturbances that depend on the operational environment such as maritime currents, wind or rough terrain. The existing MPF control laws demonstrate severe loss of performance in the presence of such disturbances and uncertainties. This warrants investigation of robust control strategies to solve the MPF control problem.

In the context of robust path following control, [12] proposes a H_∞ robust controller for ground vehicles in order to address the disturbances caused by delays and data packet dropouts. In [13], the planar path following problem was addressed by using two sliding mode controllers for both kinematic and dynamic models of the vehicle. The path function is represented explicitly, which constrains the flexibility of shape representation. Besides, the sliding

manifold for the kinematic controller is simply the angular error from an angular reference designed to steer the vehicle to the path. More recently, in [14], a sliding mode technique combined with a predictive control strategy was developed to compensate for the impact of the hydrodynamic damping coupling on a 3D path following task for an Autonomous Underwater Vehicle (AUV). In [3], a disturbance observer for constant unknown ocean currents was designed to solve the problem of dynamic positioning and way-point tracking of an underactuated AUV. The development of robust control laws for the MPF control problem has not been addressed in the literature.

This paper extends the state-of-the-art in MPF control by taking external, bounded disturbances such as unknown maritime currents into consideration through the design of robust MPF control laws. Further, we relax the assumption that the velocities of the target frame are accurately known. To this end, a Kalman filter is used to estimate the target linear and angular velocities, given the measurements of the target pose. In order to address the environmental disturbances, two variants of robust MPF control laws have been proposed. The first strategy employs a First Order Sliding Mode (FOSM) term to achieve robustness against the bounded disturbances. The second strategy seeks to directly compensate the disturbance by computing an estimate using a disturbance observer. The proposed robust control laws are proven to be Globally Asymptotically Stable with respect to the origin of a conveniently defined MPF error signal in the presence of bounded estimation errors of the target velocities and environmental disturbances. The main contributions of the paper are the design and experimental validation of two variants of robust MPF control schemes. Experimental results using Autonomous Underwater Vehicles demonstrate the viability of the proposed control schemes for applications in a real world environment.

The remainder of the paper is organized as follows. Section II formulates the MPF problem addressed with a description of the vehicle model. Section III discusses the two proposed control schemes: (i) Robust MPF control with FOSM and (ii) Robust MPF control with FOSM and a Disturbance Observer. In Section IV, the experimental results are illustrated and discussed, and finally Section V concludes the paper.

II. PROBLEM FORMULATION

A. Kinematic Model for an Underactuated Vehicle

Consider an inertial frame of reference $\{I\}$ and a body frame $\{B\}$ attached to the center of mass of the robotic vehicle, as shown in Fig. 1. The kinematic model of the vehicle moving in $\mathbf{R}^n$ with $n = 2, 3$ can be expressed by

$$\begin{aligned} \dot{p}_v(t) &= R_v(t)\, v_v + d_v \\ \dot{R}_v(t) &= R_v(t)\, S(\omega_v + d_\omega) \end{aligned} \tag{1}$$

where $p_v \in \mathbf{R}^n$ denotes the position of the robot with respect to the inertial frame $\{I\}$, $R_v \in \mathbf{SO}(n)$ denotes the rotation matrix from the body frame $\{B\}$ to frame $\{I\}$, $v_v \in \mathbf{R}^n$ and $\omega_v \in \mathbf{R}^{n(n-1)/2}$ are the linear and angular velocities of the vehicle with respect to the body frame $\{B\}$, $S(\omega_v) \in \mathbf{so}(n)$ is the skew-symmetric matrix associated to the angular velocity of the vehicle ω_v, and the signals $d_v \in \mathbf{R}^n$, $d_\omega \in \mathbf{R}^{n(n-1)/2}$ are unknown kinematic disturbances. Many different factors can be sources for these disturbances, depending on the type of robotic vehicle and the operational environment. Marine vehicles such as AUVs are affected by unknown sea conditions that can induce unwanted external velocities due to maritime currents and waves. In the case of aerial vehicles, wind and internal dynamics can induce unwanted disturbances in the kinematic model. In this work, we consider the problem of controlling an underactuated vehicle at the kinematic level, with the control signal defined as

$$u_v = \begin{bmatrix} v_f \\ \omega_v \end{bmatrix} \tag{2}$$

where the body linear velocity v_v in (1) is defined as $v_v = [\ v_f\ \ 0\ ]^\mathsf{T}$ $(n = 2)$ or $v_v = [\ v_f\ \ 0\ \ 0\ ]^\mathsf{T}$ $(n = 3)$. This is the case for vehicles where only the longitudinal velocity $v_f \in \mathbf{R}$ and the body angular velocity $\omega_v \in \mathbf{R}^{n(n-1)/2}$ can be controlled, such as some types of AUVs. We assume the existence of an inner-loop autopilot controller for the vehicle dynamics, which accurately tracks the linear and angular velocity commands generated by the controller based on the kinematic model of the robotic vehicle. Imperfect tracking by the inner-loop autopilot controller can further contribute to the velocity disturbances acting on the vehicle, that can be lumped into the terms d_v and d_ω.

B. Moving Path Following Problem

In the MPF control problem, as illustrated in Fig. 1, the vehicle is tasked to follow an *a priori* specified path expressed with respect to a moving target, which can be another vehicle performing a maneuver, a beacon or any kind of target whose position is assumed to be known or can be estimated. Define a target frame $\{T\}$ whose origin is attached to the translating and rotating target. Let $p_t(t) \in \mathbf{R}^n$ denote the position of the target with respect to the frame $\{I\}$, and $p_d^t(\gamma) \in \mathbf{R}^n$ be the desired path specified with respect to the frame $\{T\}$, parameterized by $\gamma \in \mathbb{R}$. For a given γ, p_d^t denotes the position of a virtual reference point, expressed with respect to the target frame $\{T\}$, that must be followed by the vehicle. The virtual point p_d^t and its velocity can be expressed with respect to the inertial frame as

$$p_d = p_t + R_t\, p_d^t(\gamma) \tag{3}$$

$$\dot{p}_d = v_t + R_t \left(\frac{\partial p_d^t(\gamma)}{\partial \gamma}\, \dot{\gamma} + S(\omega_t)\, p_d^t(\gamma) \right) \tag{4}$$

where $R_t \in \mathbf{SO}(n)$ is the rotation matrix of frame $\{T\}$ with respect to the inertial frame $\{I\}$, $v_t = \dot{p}_t$ is the linear velocity of the target, and $\omega_t \in \mathbf{R}^n$ is the angular velocity of the target frame, expressed in its body frame $\{T\}$.

In order to differentiate the MPF control scheme from the trajectory tracking scheme, we impose

$$\dot{\gamma} = \dot{\gamma}_d + g_{err} \tag{5}$$

where $\dot{\gamma}_d$ is the desired nominal speed of the virtual point and g_{err} is a correction signal to be defined in Section III-C. The objective of g_{err} is to explicitly control the evolution of the virtual point along the moving path, in order to enable faster convergence of the vehicle to the moving path. The robust MPF control problem can be stated as follows.

Problem (Robust Moving Path Following): Given a known pose $\{p_t, R_t\}$ of the moving target frame $\{T\}$ and the desired path $p_d^t(\gamma)$ with the speed assignment for the path parameter γ given by (5), the Robust Moving Path Following control problem is to design a control law for u_v that steers the vehicle towards the desired moving path (3) in the presence of unknown kinematic disturbances d_v, d_ω. Specifically, the goal is to control the position of the nose of the vehicle, or more generically, a point $\bar{p}_v = p_v + R_v\,\epsilon$ placed at a constant distance $\epsilon = [\,\epsilon_1\ \epsilon_2\,]^\mathsf{T}$ $(n=2)$ or $\epsilon = [\,\epsilon_1\ \epsilon_2\ \epsilon_3\,]^\mathsf{T}$ $(n=3)$ from the origin of the vehicle body frame $\{B\}$, such that the error $\bar{p}_v(t) - p_d(t)$ has a globally asymptotically stable equilibrium point at the origin. Further, it is required to satisfy the desired speed assignment $\|\dot{\gamma} - \gamma_d\| \to 0$ as $t \to \infty$.

III. ROBUST MOVING PATH FOLLOWING CONTROL

In this section, the two variants of the robust control scheme, namely Robust MPF with FOSM and Robust MPF with FOSM and Disturbance Observer are proposed to solve the MPF motion control problem.

A. Robust MPF with FOSM

The MPF error associated to the vehicle [9] is defined as

$$e_v = R_v^\mathsf{T}(\bar{p}_v - p_d) \tag{6}$$

Taking its time derivative and using (3), (4) and model (1), the error dynamics is given by

$$\begin{aligned}\dot{e}_v &= \dot{R}_v^\mathsf{T}(\bar{p}_v - p_d) + R_v^\mathsf{T}(\dot{\bar{p}}_v - \dot{p}_d)\\ &= -S(\omega_v{+}d_\omega)\,e_v + v_v + S(\omega_v{+}d_\omega)\epsilon + R_v^\mathsf{T} d_v\\ &\quad - R_v^\mathsf{T}\,v_t - R_v^\mathsf{T} R_t\left(\frac{\partial\, p_d^t}{\partial\gamma}\,\dot{\gamma} + S(\omega_t)\,p_d^t(\gamma)\right)\end{aligned}$$

Using control signal (2) with the definition of v_v yields

$$\begin{aligned}\dot{e}_v &= -S(\omega_v{+}d_\omega)\,e_v\ +\ \Delta_\epsilon u_v + d\\ &\quad - R_v^\mathsf{T}\,v_t - R_v^\mathsf{T} R_t\left(\frac{\partial p_d^t}{\partial\gamma}\,\dot{\gamma} + S(\omega_t)\,p_d^t(\gamma)\right)\end{aligned} \tag{7}$$

where Δ_ϵ is a constant matrix that can take the form

$$\Delta_\epsilon = \begin{bmatrix}1 & -\epsilon_2\\ 0 & \epsilon_1\end{bmatrix} \quad \text{or} \quad \Delta_\epsilon = \begin{bmatrix}1 & 0 & \epsilon_3 & -\epsilon_2\\ 0 & -\epsilon_3 & 0 & \epsilon_1\\ 0 & \epsilon_2 & -\epsilon_1 & 0\end{bmatrix}$$

for the planar $(n=2)$ and 3D $(n=3)$ cases, respectively. Note that it is always possible to choose ϵ such that Δ_ϵ is full rank. Vector $d \in \mathbf{R}^n$ is the total disturbance. In the planar case, it is given by

$$d = \begin{bmatrix}R_v^\mathsf{T} & s_\epsilon\end{bmatrix}\begin{bmatrix}d_v\\ d_\omega\end{bmatrix}, \quad s_\epsilon = \begin{bmatrix}-\epsilon_2\\ \epsilon_1\end{bmatrix}$$

Remark III.1. *Notice that, by the triangle inequality, the total disturbance d is bounded by $\|d\| \le \|d_v\| + \|d_\omega\|\,\|\epsilon\|$.*

Theorem 1 (Robust MPF with FOSM)**.** *Consider an underactuated robotic vehicle with dynamics described by* (1) *and control signal given by* (2)*. Let the MPF error dynamics be described by* (7)*, and consider that the configuration of the vehicle $\{p_v, R_v\} \in \mathbf{R}^n \times \mathbf{SO}(n)$ and the target frame $\{p_t, R_t\} \in \mathbf{R}^n \times \mathbf{SO}(n)$ are known. Consider also the following assumptions:*

i. Estimates of the target velocities $\hat{v}_t$, $\hat{\omega}_t$ are available.
ii. Total disturbance d and geometric path $p_d^t(\gamma)$ are bounded vector quantities.

Under these assumptions, the control law

$$\begin{aligned}u_v = \Delta_\epsilon^\dagger\Big(&-K_p\,e_v + R_v^\mathsf{T}\left(\hat{v}_t + R_t\,S(\hat{\omega}_t)\,p_d^t\right)\\ &+ R_v^\mathsf{T}\,R_t\frac{\partial p_d^t}{\partial\gamma}\dot{\gamma} - w_v\Big)\end{aligned} \tag{8}$$

ensures that the origin $e_v = 0$ of the MPF error is globally asymptotically stable. In (8)*, matrix $\Delta_\epsilon^\dagger$ is the Moore-Penrose pseudo-inverse of Δ_ϵ, $K_p \in \mathbf{R}^{n\times n}$ is a positive-definite gain matrix and w_v is a robustness term, given by*

$$w_v = \rho\,\frac{e_v}{\|e_v\|} \tag{9}$$

where ρ is a scalar designed such that

$$\rho \ge \|d_v\| + \|d_\omega\|\|\epsilon\| + \|\widetilde{v}_t\| + \|\widetilde{\omega}_t^t \times p_d^t(\gamma)\| \tag{10}$$

and $\widetilde{v}_t = v_t - \hat{v}_t$, $\widetilde{\omega}_t = \omega_t - \hat{\omega}_t$ are estimation errors on the target velocities.

Proof. Define the following Lyapunov candidate

$$V(e_v) = \frac{1}{2}\,e_v^\mathsf{T} e_v > 0 \quad \forall e_v \neq 0 \tag{11}$$

Differentiating it with respect to time and using the error dynamics in (7), yields

$$\begin{aligned}\dot{V}(e_v) &= e_v^\mathsf{T}\dot{e}_v\\ &= e_v^\mathsf{T}\Big(\Delta_\epsilon u_v + d - R_v^\mathsf{T} v_t\\ &\quad - R_v^\mathsf{T} R_t\left(\frac{\partial p_d^t}{\partial\gamma}\,\dot{\gamma} + S(\omega_t)\,p_d^t(\gamma)\right)\Big)\end{aligned} \tag{12}$$

where we have used the fact that $e_v^\mathsf{T}\,S(\omega_v{+}d_\omega)\,e_v = 0$, since $S(\omega_v + d_\omega)$ is skew-symmetric. Substituting the control law (8) in (12) yields

$$\dot{V}(e_v) = -e_v^\mathsf{T}\,K_p\,e_v + e_v^\mathsf{T}\left(D - \rho\,\frac{e_v}{\|e_v\|}\right)$$

where $D = d - R_v^\mathsf{T}\left(\widetilde{v}_t + R_t\,S(\widetilde{\omega}_t)\,p_d^t\right)$. Since $K_p > 0$, the first term is negative definite. Conversely, using the Cauchy-Schwarz inequality, the second term is bounded by

$$e_v^\mathsf{T}\,(D - w_v) = e_v^\mathsf{T} D - \rho\|e_v\| \le \|e_v\|\,(\|D\| - \rho) \tag{13}$$

By Remark III.1 and using the triangle inequality, note that $\|D\|$ is bounded by the quantity on the right-hand side of (10). Therefore, if Assumptions (i), (ii) are satisfied, it

is always possible to choose ρ such that (10) is valid. In these conditions, $\rho \geq \|D\|$ and $e_v^{\mathsf{T}}(D - w_v)$ is negative semi-definite by (13), making $\dot{V}(e_v)$ negative definite. Since $V(e_v) \to \infty$ when $\|e_v\| \to \infty$, the origin $e_v = 0$ is globally asymptotically stable. □

Using the concept of Filippov solutions for discontinuous differential equations [15], it is possible to show that (9) has an infinite switching frequency in the origin $e_v = 0$. In practice, this frequency is finite due to nonlinear effects and hardware limitations, but small values for $\|e_v\|$ in the denominator can cause numerical issues and chattering phenomena. To avoid this problem, (9) can be implemented as

$$w_v = \begin{cases} \rho \frac{e_v}{\|e_v\|} & , \quad \|e_v\| \geq \epsilon_w \\ \rho \frac{e_v}{\epsilon_w} & , \quad \|e_v\| < \epsilon_w \end{cases} \tag{14}$$

where ϵ_w is a positive scalar. In this case, it is not possible to demonstrate asymptotic stability, but it is possible to guarantee that $\|e_v\|$ is bounded around the origin [16].

B. Robust MPF with Disturbance Observer

In the presence of large amplitude disturbances, it may be difficult to tune the parameters ρ and ϵ_w so as to satisfy (10) while reducing the chattering in the control inputs. In these situations, an observer can be designed to provide an estimate of the disturbance. Furthermore, this estimate can be used in the control law to actively compensate the disturbance.

Without loss of generality, consider the planar problem, wherein the vehicle pose $\{p_v, R_v\} \in \mathbf{R}^2 \times \mathbf{SO}(2)$ is known and the vehicle orientation is parameterized by the heading angle $\psi \in \mathbf{R}$, such that $R_v = R_v(\psi) \in \mathbf{SO}(2)$. Then, the disturbance observer for the translational disturbance is defined as

$$\begin{cases} \dot{\hat{p}}_v = R_v\, v_v + \hat{d}_v + K_1\, \widetilde{p}_v \\ \dot{\hat{d}}_v = K_2\, \widetilde{p}_v \end{cases} \tag{15}$$

where the estimation errors $\widetilde{p}_v = p_v - \hat{p}_v$, $\widetilde{d}_v = d_v - \hat{d}_v$ and the vehicle position p_v are measured. For positive-definite gains $K_1, K_2 \in \mathbf{R}^{2\times 2}$, the estimation errors $\widetilde{p}_v$, $\widetilde{d}_v$ can be proven to be asymptotically stable at the origin [17].

An observer for the rotational disturbance d_ω can be designed as

$$\begin{cases} \dot{\hat{\psi}} = \omega_v + \hat{d}_\omega + k_{\omega_1}\widetilde{\psi} \\ \dot{\hat{d}}_\omega = k_{\omega_2}\widetilde{\psi} \end{cases} \tag{16}$$

where the estimation errors are defined as $\widetilde{\psi} = \psi - \hat{\psi}$ and $\widetilde{d}_\omega = d_\omega - \hat{d}_\omega$, and the vehicle planar orientation ψ is measured. Similarly, for positive gains $k_{\omega_1}, k_{\omega_2} \in \mathbf{R}$, the estimation errors $\widetilde{\psi}$, $\widetilde{d}_\omega$ can be proven to be asymptotically stable at the origin.

Theorem 2 (Robust MPF with Disturbance Observer)**.** *Consider an underactuated robotic vehicle under the assumptions of Theorem 1. The control law* (8) *with w_v redefined as*

$$\overline{w}_v = \rho\, \frac{e_v}{\|e_v\|} + \hat{d}\,, \quad \hat{d} = \begin{bmatrix} R_v^{\mathsf{T}} & s_\epsilon \end{bmatrix} \begin{bmatrix} \hat{d}_v \\ \hat{d}_\omega \end{bmatrix} \tag{17}$$

ensures that the origin $e_v = 0$ of the MPF error is globally asymptotically stable, where ρ is a scalar designed such that

$$\rho \geq \|\widetilde{d}_v\| + \|\widetilde{d}_\omega\|\|\epsilon\| + \|\widetilde{v}_t\| + \|\widetilde{\omega}_t^t \times p_d^t(\gamma)\| \tag{18}$$

Proof. The proof follows steps similar to the proof of Theorem 1 with the candidate Lyapunov function $V = \frac{1}{2} e_v^{\mathsf{T}} e_v$. Using the error dynamics (7) with control laws (8) and (17), the time-derivative of the Lyapunov function is

$$\dot{V}(e_v) = -e_v^{\mathsf{T}}\, K_p\, e_v + e_v^{\mathsf{T}} \left(\widetilde{D} - \rho\, \frac{e_v}{\|e_v\|} \right)$$

where $\widetilde{D} = \widetilde{d} - R_v^{\mathsf{T}}\left(\widetilde{v}_t + R_t\, S(\widetilde{\omega}_t)\, p_d^t\right)$ and $\widetilde{d}$ is the total estimation error, given by $\widetilde{d} = d - \hat{d}$. As before, using the Cauchy-Schwarz inequality, the second term is bounded by

$$e_v^{\mathsf{T}}\,(\widetilde{D} - w_v) = e_v^{\mathsf{T}}\widetilde{D} - \rho\|e_v\| \leq \|e_v\|\,(\|\widetilde{D}\| - \rho) \tag{19}$$

By Remark III.1 and the triangle inequality, note that $\|\widetilde{D}\|$ is bounded by the quantity on the right-hand side of (18). Therefore, if Assumptions (i) and (ii) of Theorem 1 are satisfied, it is always possible to choose ρ such that (18) is valid. In these conditions, $\rho \geq \|\widetilde{D}\|$ and $e_v^{\mathsf{T}}(\widetilde{D} - w_v)$ is negative semi-definite by (13), making $\dot{V}(e_v)$ negative definite. Since $V(e_v) \to \infty$ when $\|e_v\| \to \infty$, the origin $e_v = 0$ is globally asymptotically stable. □

Remark III.2. *Note that according to* (18)*, the sliding mode gain ρ must overcome only the norm of the disturbance estimation errors instead of the total norm of the disturbance, as in* (10)*. If the disturbance observer is properly designed, this reduces the amount of chattering in the control inputs.*

Remark III.3. *Using the induced norm for square matrices, $\|A\| = \sup\{\|Ax\| : x \in \mathbb{R}^n$ with $\|x\| = 1\}$, with $A \in \mathbb{R}^{n\times n}$, it is possible to derive explicit bounds for the norm of $\|u_v\|$ during the steady state ($e_v = 0$):*

$$\|u_v\| \leq \|\Delta_\epsilon^\dagger\| \left(\|\hat{v}_t\| + \|\hat{\omega}_t \times p_d^t\| + \left\| \frac{\partial p_d^t}{\partial \gamma} \right\| |\dot{\gamma}| + \rho + \|\hat{d}\| \right)$$

Considering velocity actuation limits of the form $\|u_v\| \leq u_{max}$, the maximum actuation norm u_{max} must be greater or equal the value on the right-hand side of this inequality, so that the control input u_v is kept inside the actuation limits during the steady state. A similar remark can be made for the previous controller, considering $\hat{d} = 0$.

Controller (8) differs from the works [9], [11] by the robustness terms (9) or (17) and by taking the target frame rotation into account on (3). That is, those works do not address the problem of robustness in the presence of kinematic disturbances, rotating target frames and also consider

the target velocity v_t to be known, an assumption that was relaxed in our work. Furthermore, [9] does not consider the design of the error correction term g_{err} term (presented in Section III-C) in the path dynamics (5) to achieve faster convergence of the vehicle to the moving path.

C. Path variable dynamics

As mentioned previously, imposing the dynamics (5) on the path variable γ allows to explicitly control the progression of the virtual point p_d along the moving path. This can be done using the previously defined error correction term $g_{err}(t)$, that can be designed to delay or to stop the evolution of the path variable γ if the vehicle is too far away from the path. Using the gradient of the path error (6) squared with respect to the path variable

$$\eta_v = \frac{\partial(\frac{1}{2}e_v^{\mathsf{T}}e_v)}{\partial\gamma} = -e_v^{\mathsf{T}}\, R_v^{\mathsf{T}}\, R_t \left(\frac{\partial p_d^t(\gamma)}{\partial\gamma}\right) \qquad (20)$$

we can define $g_{err} = -k_\eta\, sat(\eta_v)$ for some $k_\eta > 0$. The saturation function guarantees the boundedness for the correction term. Its effect is to effectively delay the evolution of the virtual point along the path by explicitly avoiding the evolution of γ if the MPF error norm is too large. Besides, to ensure that the effect of g_{err} will overcome the evolution of γ when needed, it suffices to choose $k_\eta \geq \dot{\gamma}_d$.

IV. EXPERIMENTAL RESULTS

A. Experimental Setup

The experiments were performed on Porto de Leixões (Porto, Portugal) using a Light Autonomous Underwater Vehicle (LAUV) from the Underwater Systems and Technology Laboratory (LSTS) at the Faculty of Engineering of the University of Porto (FEUP). A LAUV is a portable and lightweight vehicle that can be easily launched, operated and recovered. The AUV operates under the DUNE and Neptus environments, which are part of a software toolchain [18] developed at LSTS. DUNE is the on-board software running on the vehicles, comprising all the software needed for communications, navigation, control, maneuvering, plan execution and supervision of multiple types of robotic vehicles. The control algorithms were implemented using C++, on DUNE. Neptus is the software used for command and control of the AUV, comprising many typical functions needed for a typical mission, such as planning, execution and post-mission analysis.

A simulated vehicle was used as a target, whereas the AUV was used to perform the MPF task around the target, as shown in Figure 2. The target vehicle performs a loiter maneuver with the radius of $60\,m$ in the counter-clockwise direction and continuously transmits its position (computed from GPS measurements) over Wi-Fi to the AUV, which executes the MPF control law. The control algorithm for the target vehicle is a vector field method [19]. The desired path for the AUV is a circle centered at the target with the radius of $25\,m$. More precisely, it is parameterized by

$$p_d^t(\gamma) = R \begin{bmatrix} \cos(\gamma/R) \\ \sin(\gamma/R) \end{bmatrix}$$

Fig. 2. Neptus console. Simulated target follows a loitering maneuver while the LAUV executes the Robust MPF controllers.

where $R = 20\,m$. Note that, in this particular case, $\|\partial p_d^t(\gamma)/\partial\gamma\| = 1\ \forall\gamma$, which means that the path variable γ coincides with the path arc length. For the construction of the path error e_v, the value $\epsilon = \begin{bmatrix}1 & 0\end{bmatrix}^{\mathsf{T}}$ was used. The controller gain matrix was chosen as $K_p = diag(0.2, 0.2)$. The gain for the error correction term was chosen as $k_\eta = 4$, and the desired nominal speed of the virtual point is $\dot{\gamma}_d = 1\,m/s$.

B. Kalman Filter for Target Velocity Estimation

To achieve accurate estimates for the target velocities, a linear Kalman filter was designed. Considering the planar case, the target can be approximated as a moving rigid body with a constant velocity, while its acceleration is considered as a random variable drawn from a Gaussian distribution. Under this assumption, the target is modeled as

$$\dot{p}_t = v_t\,, \qquad \dot{v}_t = a_t$$
$$\dot{\psi}_t = \omega_t\,, \qquad \dot{\omega}_t = \alpha_t$$

where ψ_t is the heading angle of the target, and a_t, α_t are the target linear and angular accelerations drawn from Gaussian distributions with zero mean and covariances $\Sigma_p^2 = diag(0.1, 0.1)$, $\sigma_p^2 = 10^{-4}$, respectively. This linear model can be discretized using a zero order hold (ZOH), yielding a discrete linear, time-invariant model whose states are the target position, angle and velocities at each sample time. The measured outputs are the target position and orientation angle, sent through Wi-Fi to the AUV with a frequency of $1Hz$.

The Kalman filter is implemented according to the *predict/update* strategy. Every sampling instant, a new prediction of the target pose and velocities are computed, and the update step is computed when a new Wi-Fi message containing a position/angle measurement is received from the simulated target vehicle. If no data from the simulated target is received for more than $10\,s$, the vehicle considers p_t to be fixed at the last position received and $\hat{v}_t = 0$. The measurement noise covariances were chosen as $\Sigma_m^2 = diag(0.1, 0.1)$ and

$\sigma_m^2 = 10^{-4}$. The initial target state covariances are: $2m$ for the position, $1\,rad$ for the orientation, $0.1\,m/s$ and $0.1\,rad/s$ for the linear and angular velocities.

C. Experimental Results

First, we present the results obtained by using the nominal MPF controller with no robustness term ($\rho = 0$) from [9], [11] that forms the base controller for performance evaluation of the proposed robust MPF schemes. The network router

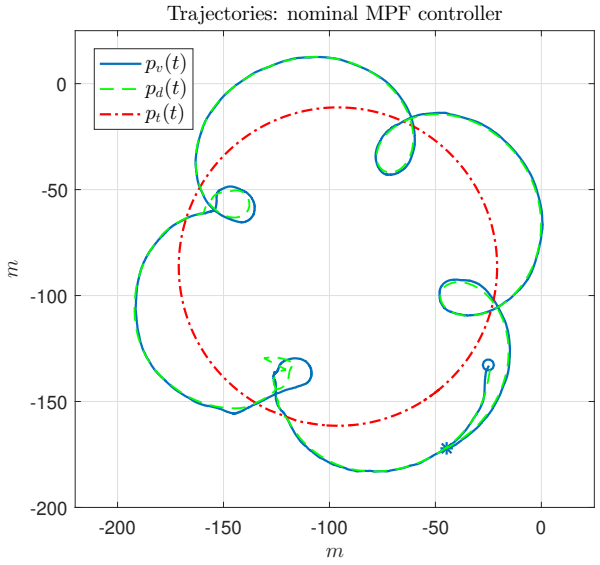

Fig. 3. Trajectories using the nominal MPF controller.

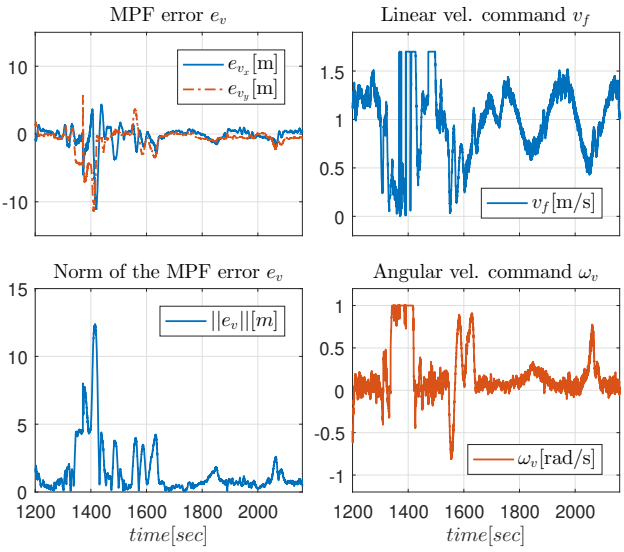

Fig. 4. Results for the nominal MPF controller.

was located on the northeast part of Fig. 3, close to the origin of the inertial frame. Data loss can be noticed in the trajectory of p_d on the distant southwest side on Fig. 3, where the vehicle failed to receive the position of the target for a couple of moments due to the distance from the router. This can be noticed in the MPF error shown in Fig. 4, around the time mark of $1400\,s$. Thereafter, the norm of the MPF error remains bounded by $3\,m$. The velocity control commands reach saturation during the transient and on occasional moments of communication losses, but remain within the actuation limits during most of the experiment (see Remark III.3).

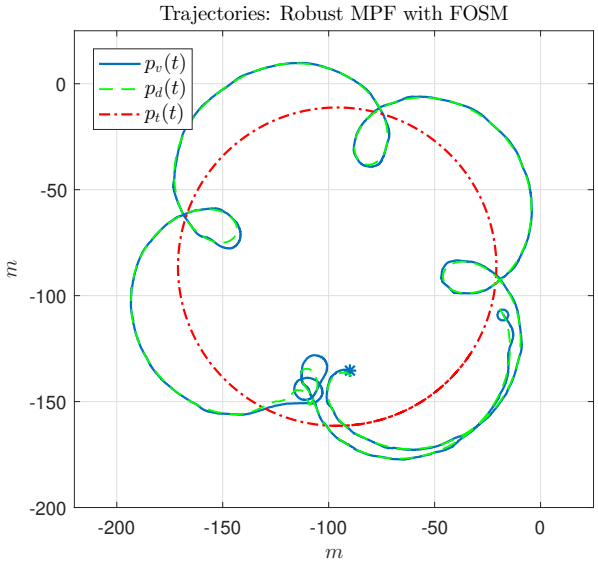

Fig. 5. Trajectories using the Robust MPF controller with FOSM term (RMPF-FOSM).

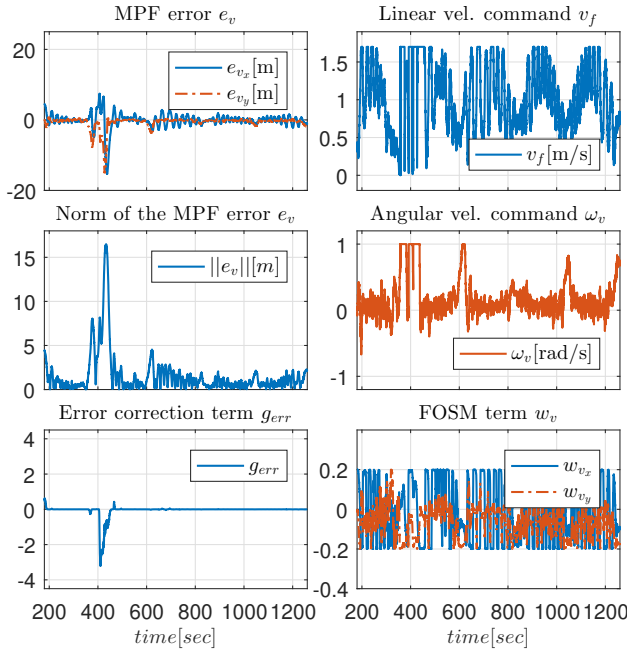

Fig. 6. Results for the Robust MPF controller with FOSM term (RMPF-FOSM).

Figure 5 shows the vehicle trajectory obtained with the Robust MPF controller with FOSM (Theorem 1) with $\rho = 0.2$ and $\epsilon_w = 0.5$. Figure 6 illustrates the MPF error and

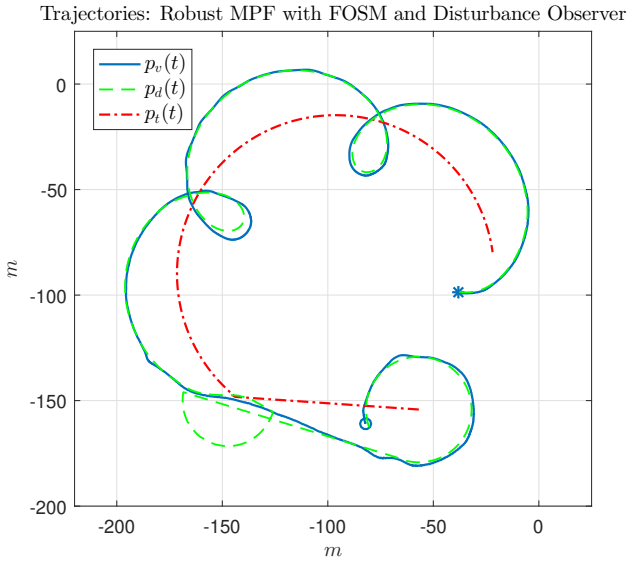

Fig. 7. Trajectories using the Robust MPF controller with FOSM term and Disturbance Observer (RMPF-FOSM-DO).

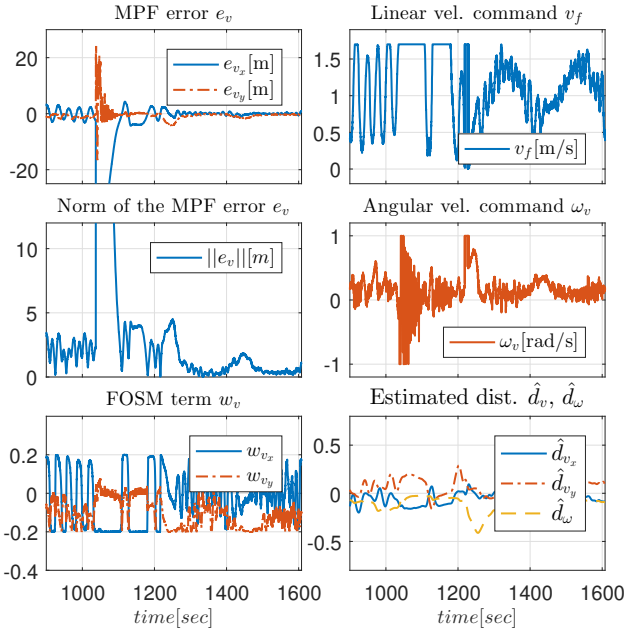

Fig. 8. Results for the Robust MPF controller with FOSM term and Disturbance Observer (RMPF-FOSM-DO).

the generated control signals. The norm of the MPF error remains bounded by less than $2\,m$, unless on the farthest point from the router, where loss of data packages was observed. The MPF error converges to a neighborhood of the origin due to the implementation of the control law using (8) and (14). As expected, chattering was observed in the linear and angular velocity commands. However, the control signals remain within their actuation limits, inducing a practical sliding mode behavior in the MPF error, as observed in Fig. 6. The norm of the MPF error is smaller for the robust MPF with FOSM scheme. The dynamics during sliding ($e_v = 0$) is *invariant* to disturbances bounded by ρ, provided that (10) is satisfied. Lastly, note the action of the error correction term g_{err} during the moment around $400\,s$ where communications were lost. It controls the progression of the virtual point along the moving path in order to enable faster convergence of the AUV. Once the MPF error starts to grow, g_{err} slows down the evolution of γ, effectively waiting until the vehicle is able to follow the path.

Figures 7 and 8 show the results for the Robust MPF with FOSM and Disturbance Observer (Theorem 2) with $\rho = 0.2$ and $\epsilon_w = 0.5$. The gains for the disturbance observer were obtained using the pole placement method such that the desired observer response is critically damped with approx. $20\,s$ of rising time. It is evident from Fig. 7 that this experiment suffered significant losses in the communications, with no data being received by the AUV during several minutes until the network was restored near the point $\{-150\,m, -150\,m\}$. In this case, since no data from the target was received for more than $10\,s$, the follower vehicle considers p_t to be fixed, resulting in a stationary circular maneuver around the point $\{-150\,m, -50\,m\}$. After the communications were re-established around the time mark of $1250\,s$, the MPF error converges to the origin with a significantly smaller norm than in the classical MPF (Fig. 4) and in the Robust MPF with FOSM (Fig. 6), thereby demonstrating superior, robust performance over the nominal MPF control scheme. There is an evident reduction on the chattering level on the control signals when compared to the Robust MPF with FOSM (Fig. 6), which is a consequence of the use of the disturbance estimators along with the FOSM term, as mentioned in Remark III.2. The improvement in the chattering levels can also be noticed from the FOSM term signal w_v in Fig. 8. The components of the estimated disturbances $\hat{d}_v$ and $\hat{d}_\omega$ are shown in Fig. 8.

D. Simulation Results

This section presents simulation results in order to facilitate comparisons between the proposed robust MPF control laws and the nominal MPF control. These simulations were performed in the hardware-in-the-loop setup, where the simulation parameters were set identical to the experiments. Constant maritime currents of $0.1\,m/s$ to the North and East were simulated. DUNE has an in-built simulator that simulates sensor and actuator dynamics, as well as the dynamic model of the AUV. The control commands generated by the MPF controllers are provided as velocity inputs to the detailed dynamic model.

Figure 9 shows a comparison between the nominal MPF controller ($\rho = 0$) and the proposed robust MPF schemes. The value $\rho = 0.2$ is the same as the one used in the experiments and is enough to overcome the norm of the total disturbance due to the simulated maritime currents (see inequality (10)). Notice how the norm of the MPF error in the robust MPF schemes is noticeably smaller than in the nominal MPF controller, and how the chattering level in simulation is much smaller than the value obtained in practice. This is expected because the chattering performance

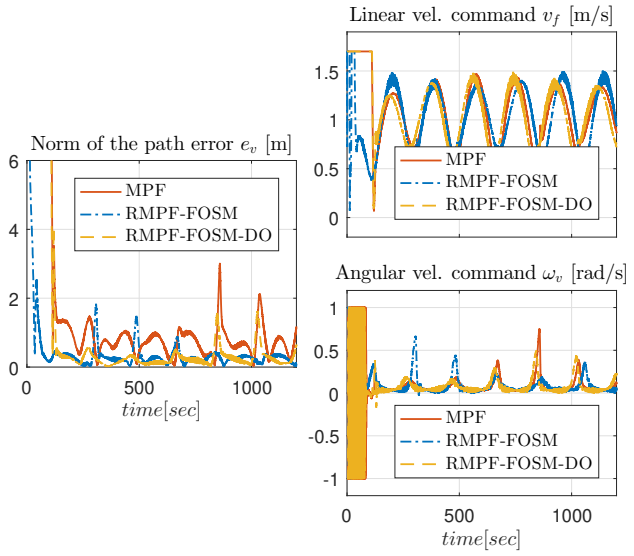

Fig. 9. Comparison between the nominal MPF and the proposed Robust MPF schemes.

of sliding mode-based controllers tend to degrade when *unmodeled dynamics* are present in the control channel [20]. Furthermore, the amount of chattering in the control inputs in the Robust MPF with FOSM and Disturbance Observer (RMPF-FOSM-DO) is indeed smaller than in the Robust MPF with FOSM (RMPF-FOSM) scheme (see Remark III.2), the same result observed in the experiments.

V. CONCLUSIONS

This work addressed the Robust MPF problem for underactuated vehicles, such as an AUV. Two robust MPF control schemes were proposed, ensuring asymptotic stability of the origin of the MPF error in the presence of bounded disturbances acting on the vehicle and inaccurate estimates for the target velocities. The proposed control schemes were validated experimentally using an AUV and it was demonstrated that their performance is superior over the nominal MPF control technique. Additionally, it was observed that the use of disturbance observers for active compensation of the bounded kinematic disturbances can reduce the level of chattering on the control signals by reducing the total amount of disturbance that the FOSM term must compensate. Satisfactory performance was achieved in the presence of unmodeled dynamics of the inner-loop controller for the actuators and unknown kinematic disturbances acting on the vehicle.

ACKNOWLEDGMENTS

The authors would like to acknowledge the support of the LSTS staff in conducting the experiments on Porto de Leixões. The code used in the experiments can be accessed from the GITHUB® account on `https://github.com/CaipirUltron/dune`. The video to the experiments can be found at `https://www.youtube.com/playlist?list=PLjRBDQmzSDGR5oGz3gXoTJvpQzolYKIkz`.

REFERENCES

[1] C. Samson, "Path following and time-varying feedback stabilization of a wheeled mobile robot," *Second International Conference on Automation, Robotics and Computer Vision*, vol. 3, 01 1992.

[2] A. Micaelli and C. Samson, "Trajectory tracking for unicycle-type and two-steering-wheels mobile robots," Ph.D. dissertation, INRIA, 1993.

[3] A. P. Aguiar and J. P. Hespanha, "Trajectory-tracking and path-following of underactuated autonomous vehicles with parametric modeling uncertainty," *IEEE Transactions on Automatic Control*, vol. 52, no. 8, pp. 1362–1379, Aug 2007.

[4] D. Soetanto, L. Lapierre, and A. Pascoal, "Adaptive, non-singular path-following control of dynamic wheeled robots," in *Decision and Control, 2003. Proceedings. 42nd IEEE Conference on*, vol. 2. IEEE, 2003, pp. 1765–1770.

[5] A. P. Aguiar, J. P. Hespanha, and P. V. Kokotovic, "Path-following for nonminimum phase systems removes performance limitations," *IEEE Transactions on Automatic Control*, vol. 50, no. 2, pp. 234–239, Feb 2005.

[6] T. Oliveira and P. Encarnação, "Ground target tracking control system for unmanned aerial vehicles," *Journal of Intelligent & Robotic Systems*, vol. 69, no. 1-4, pp. 373–387, 2013.

[7] T. Oliveira, A. P. Aguiar, and P. Encarnação, "Moving path following for unmanned aerial vehicles with applications to single and multiple target tracking problems," *IEEE Transactions on Robotics*, vol. 32, no. 5, pp. 1062–1078, Oct 2016.

[8] T. Oliveira, A. P. Aguiar, and P. Encarnação, "Three dimensional moving path following for fixed-wing unmanned aerial vehicles," in *2017 IEEE International Conference on Robotics and Automation (ICRA)*, May 2017, pp. 2710–2716.

[9] R. P. Jain, A. Alessandretti, A. P. Aguiar, and J. B. De Sousa, "Cooperative moving path following using event based control and communication," in *2018 13th APCA International Conference on Automatic Control and Soft Computing (CONTROLO)*, June 2018, pp. 189–194.

[10] Y. A. Kapitanyuk, H. G. de Marina, A. V. Proskurnikov, and M. Cao, "Guiding vector field algorithm for a moving path following problem," *IFAC-PapersOnLine*, vol. 50, no. 1, pp. 6983 – 6988, 2017, 20th IFAC World Congress.

[11] R. P. K. Jain, A. P. Aguiar, A. Alessandretti, and J. Borges de Sousa, "Moving path following control of constrained underactuated vehicles: A nonlinear model predictive control approach," in *AIAA SciTech Forum*. American Institute of Aeronautics and Astronautics, Jan 2018.

[12] R. Wang, H. Jing, C. Hu, F. Yan, and N. Chen, "Robust H_∞ path following control for autonomous ground vehicles with delay and data dropout," *IEEE Transactions on Intelligent Transportation Systems*, vol. 17, no. 7, pp. 2042–2050, July 2016.

[13] O. H. Dagci, U. Y. Ogras, and U. Ozguner, "Path following controller design using sliding mode control theory," in *Proceedings of the 2003 American Control Conference, 2003.*, vol. 1, June 2003, pp. 903–908 vol.1.

[14] L.-J. Zhang, H.-M. Jia, and D.-P. Jiang, "Sliding mode prediction control for 3d path following of an underactuated auv," *IFAC Proceedings Volumes*, vol. 47, no. 3, pp. 8799 – 8804, 2014, 19th IFAC World Congress.

[15] T. Ito, "A filippov solution of a system of differential equations with discontinuous right-hand sides," *Economics Letters*, vol. 4, no. 4, pp. 349 – 354, 1979.

[16] B. Siciliano, L. Sciavicco, L. Villani, and G. Oriolo, *Robotics: Modelling, Planning and Control*, 1st ed. Springer Publishing Company, Incorporated, 2008.

[17] A. P. Aguiar and A. M. Pascoal, "Dynamic positioning and way-point tracking of underactuated auvs in the presence of ocean currents," in *Proceedings of the 41st IEEE Conference on Decision and Control, 2002.*, vol. 2, Dec 2002, pp. 2105–2110 vol.2.

[18] J. Pinto, P. S. Dias, R. Martins, J. Fortuna, E. Marques, and J. Sousa, "The lsts toolchain for networked vehicle systems," in *2013 MTS/IEEE OCEANS-Bergen*. IEEE, 2013, pp. 1–9.

[19] D. R. Nelson, D. B. Barber, T. W. McLain, and R. W. Beard, "Vector field path following for miniature air vehicles," *IEEE Transactions on Robotics*, vol. 23, no. 3, pp. 519–529, June 2007.

[20] Y. Shtessel, C. Edwards, L. Fridman, and A. Levant, *Sliding Mode Control and Observation*, 1st ed. Springer, 2014.